Oscillatory interlayer exchange coupling in $[Pt/Co]_n/NiO/[Co/Pt]_n$ multilayers with perpendicular anisotropy: Dependence on NiO and Pt layer thicknesses

Z. Y. Liu,[1] Lanping Yue,[1] D. J. Keavney,[2] and S. Adenwalla[1,*]
[1]*Department of Physics and Astronomy and Center for Materials Research and Analysis (CMRA), University of Nebraska-Lincoln, Lincoln, NE 68588-0111, USA*
[2]*Advanced Photon Source, Argonne National Lab, Argonne, Illinois 60439, USA*
(Received 17 September 2003; revised manuscript received 29 July 2004; published 17 December 2004)

Interlayer exchange coupling has been studied in a series of $[Pt(t_{Pt}\ Å)/Co(4\ Å)]_n/NiO(t_{NiO})/[Co(4\ Å)/Pt(t_{Pt}\ Å)]_n$ multilayers with perpendicular anisotropy. The coupling oscillates between antiferromagnetic and ferromagnetic as a function of t_{NiO} with a period of ~5 Å, and the oscillatory behavior is related to the antiferromagnetic ordering of the NiO layer. This interlayer coupling between two Co/Pt multilayers is shown to occur domain by domain by magnetic force microscopy imaging. For the strongest antiferromagnetic coupling at $t_{NiO}=11$ Å, an oscillation with a period of ~6 Å is superposed onto the exponential decay of the coupling strength as a function of t_{Pt}. The exponential decay with t_{Pt} is ascribed to the exponential decay of the coupling between the Co layers across the Pt layers in each Co/Pt multilayer, and the superposed oscillatory behavior can be attributed to multiple reflections of electron waves at the Co/Pt interfaces and their interference. A linear dependence of the antiferromagnetic coupling strength on $1/n$, (where n is the number of repeats), is suggestive of a surface interaction for this interlayer coupling.

DOI: 10.1103/PhysRevB.70.224423 PACS number(s): 75.70.Cn, 75.30.Gw, 75.30.Et, 75.70.Ak

I. INTRODUCTION

Since the first observation of an antiferromagnetic (AF) interlayer exchange coupling between Fe layers with in-plane anisotropy separated by a Cr spacer,[1] interlayer exchange coupling (IEC) has been observed experimentally for a wide variety of spacer materials such as nonmagnetic metals (Ru, Cu, Au, Mo, Pd, etc.),[2–10] antiferromagnetic (AF) metals (Cr, Mn),[2,11–17] insulating (MgO)[18,19] and semiconducting (Si, ZnAs, etc.)[20–22] materials.

For nonmagnetic metallic spacers, an oscillatory IEC has been observed as a function of the spacer thickness in almost all cases (Ref. 23, and references therein). For AF metallic Cr spacers, IEC oscillations with increasing Cr thickness have been found in sputtered Fe(Co)/Cr multilayers[2,11] and epitaxial Fe/Cr/Fe sandwiches.[12–15] In the epitaxial case,[13] two oscillatory periods are observed- a short-period oscillation of 2 ML is superposed on a long-period oscillation of 18 ML. For a Mn spacer in Fe/Mn/Fe systems,[16,17] oscillatory IEC with a period of 2 ML has also been observed. According to the proximity magnetism model by Slonczewski,[24] this interlayer coupling originates from the direct exchange coupling at the ferromagnetic/Cr(Mn) interfaces and propagates through the magnetic ordering of the Cr(Mn) spacer via short-range exchange interactions.

Antiferromagnetic IEC has also been observed for insulating spacers such as MgO[18,19] and semiconducting spacers such as Si.[20,21] However, the coupling strength has been found to decay monotonically with increasing spacer thickness,[19,20] and increase with increasing temperature[21] in contrast to the case for metallic spacers.

For metallic spacers, the oscillation of the coupling strength is attributed to the spacer metal Fermi surface. The oscillatory period is related to spanning vectors of the Fermi surface lying perpendicular to the layer plane,[25,26] and the coupling arises from Ruderman–Kittel–(Kasuya)–Yosida-type coupling. In the quantum interference model by Bruno,[27] the concept of a complex Fermi surface is proposed for the insulating spacer, and a generalization of the model to insulating spacers has shown that the coupling strength should show a nonoscillatory decay with increasing insulating spacer thickness and increase with increasing temperature, being consistent with experimental observations. From the quantum interference model, it is also expected that the coupling strength across a metallic spacer oscillates as a function of the ferromagnetic layer thickness, which has been confirmed experimentally.[28,29]

Recently, coexistence of exchange biasing and ferromagnetic interlayer coupling between two ferromagnetic layers with in-plane anisotropy separated by NiO spacers has been reported.[30,31] In NiFe/NiO/Co trilayers,[31] a 90° coupling has been observed between NiFe and Co layers, and the coupling exists for a NiO thickness up to 25 nm.

Most studies on the IEC have concentrated on ferromagnetic layers with in-plane anisotropy. IEC has also been reported between ferromagnetic (FM) layers with out-of-plane anisotropy separated by metallic spacers in Co/Ru[32,33] and Ni/Cu[34] superlattices. However, observations of interlayer coupling between FM layers with perpendicular anisotropy separated by insulating spacers are scarce. Recently, we have reported an observation of interlayer coupling between two Co/Pt multilayers with perpendicular anisotropy separated by NiO spacer layers.[35] The coupling oscillates between antiferromagnetic and ferromagnetic as a function of the NiO thickness, and the antiferromagnetic coupling strength increases with increasing temperature.

In this work, detailed investigations have been performed on the interlayer coupling in $[Pt(t_{Pt}\ Å)/Co(4\ Å)]_n/NiO(t_{NiO}Å)/[Co(4\ Å)/Pt(t_{Pt}\ Å)]_n$ multilayers. The manuscript is organized as follows. Sample preparation and ex-

perimental measurements are described in Sec. II. Experimental results and discussions regarding the variation of the IEC with t_{NiO}, t_{Pt}, and n and are presented in Sec. III. Section IV presents a summary of the results obtained.

II. SAMPLE PREPARATION AND EXPERIMENTAL MEASUREMENTS

All samples were prepared by dc and rf magnetron sputtering from separate Pt, Co, and NiO targets at deposition rates of 0.96, 0.2, and 0.19 Å/s, respectively, in 3 mTorr Ar pressure. The base pressure was 4×10^{-7} Torr. In each run, up to 12 samples can be grown under identical conditions. Four sets of samples were grown in four separate runs, which are listed as follows:

S1: Glass/Pt(100 Å)/$[$Pt(5 Å)/Co(4 Å)$]_3$/NiO(t_{NiO} Å)/ $[$Co(4 Å)/Pt(5 Å)$]_3$/Pt(50 Å)

where 8 Å; $<t_{NiO}<$ 24 Å;

S2: Glass/Pt(100 Å)/$[$Pt(5 Å)/Co(4 Å)$]_4$/NiO(t_{NiO} Å)/ $[$Co(4 Å)/Pt(5 Å)$]_4$/Pt(50 Å)

where 8 Å; $<t_{NiO}<$ 26 Å;

S3: Glass/Pt(100 Å)/$[$Pt(t_{Pt} Å)/Co(4 Å)$]_4$/NiO(11 Å)/ $[$Co(4 Å)/Pt(t_{Pt} Å)$]_4$/Pt(50 Å)

where 5 Å$<t_{Pt}<$ 20 Å;

S4: Glass/Pt(100 Å)/$[$Pt(5 Å)/Co(4 Å)$]_n$/NiO(11 Å)/ $[$Co(4 Å)/Pt(5 Å)$]_n$/Pt(50 Å)

where $2<n<6$.

Three additional samples of

glass/Pt(100 Å)/$[$Pt(5 Å)/Co(4 Å)$]_3$/NiO(11 Å),

glass/NiO(11 Å)/$[$Co(4 Å)/Pt(5 Å)$]_3$/Pt(50 Å),

glass/Pt(100 Å)/$[$Pt(5 Å)/Co(4 Å)$]_3$/Pt(20 Å)

were also grown to check the effect of the NiO layer on the coercivity of Co/Pt multilayers.

The thickness calibration was checked by grazing angle x-ray reflectivity after sample preparation, displaying an accuracy of ~10%. The sample structure was checked by x-ray diffraction. Figure 1 shows the x-ray diffraction result for one sample with a NiO thickness of 11 Å in S1. The Pt layers are polycrystalline, but are highly fcc (111) textured; the Co layers are highly hcp(100) textured, and the NiO layer is highly fcc(111) textured. X-ray absorption spectroscopy (XAS) data taken on similar samples with identical hysteresis loops indicate that the Co layers are not oxidized and that the NiO layer is indeed consistent with Ni being in the +2 valence state.[36] Neither the L3 nor the L2 edge for Co show any splitting, whereas the L2 edge for Ni shows clear evidence of splitting.

Magnetic force microscopy (MFM) imaging was performed on the as-grown samples to obtain the domain patterns using low-magnetic-stray-field and high-coercivity MFM tips, with magnetization perpendicular to the sample surface.

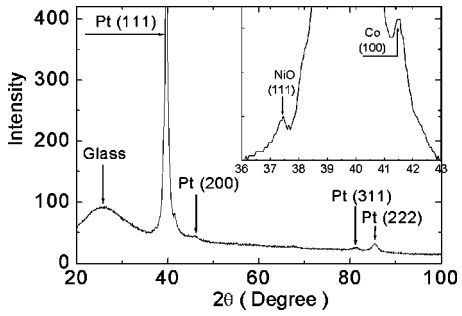

FIG. 1. X-ray diffraction result for glass/Pt(100 Å)/ $[$Pt(5 Å)/Co(4 Å)$]_3$/NiO(11 Å)/$[$Co(4 Å)/Pt(5 Å)$]_3$/Pt(50 Å), which shows that both the Pt and NiO layers are highly fcc(111) textured, and the Co layers are highly hcp(100) textured.

Hysteresis loops have been measured by a superconducting quantum interference device (SQUID) and/or an alternating gradient force magnetometer (AGFM) with the field applied perpendicular to the sample surface.

All x-ray magnetic circular dichroism (XMCD) and XAS data were taken at the beam line 4IDC at the Advanced Photon Source at Argonne National Lab.

III. RESULTS AND DISCUSSION

A. Effect of NiO layer on coercivity

Figure 2 displays the hysteresis loops for the three samples of glass/Pt(100 Å)/$[$Pt(5 Å)/Co(4 Å)$]_3$/Pt(20 Å), glass/Pt(100 Å)/$[$Pt(5 Å)/Co(4 Å)$]_3$/NiO(11 Å), and glass/NiO(11 Å)/$[$Co(4 Å)/Pt(5 Å)$]_3$/Pt(50 Å). All three loops were measured at room temperature using AGFM with the field applied perpendicular to the sample surface. The square loop shapes are suggestive of out-of-plane easy

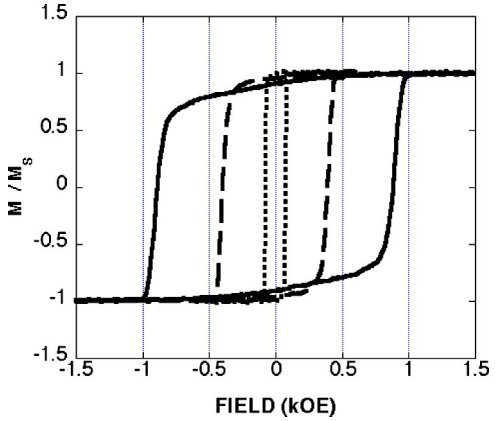

FIG. 2. Hysteresis loops at room temperature for the samples of glass/Pt(100 Å)/$[$Pt(5 Å)/Co(4 Å)$]_3$/NiO(11 Å) (solid line), glass/NiO(11 Å)/$[$Pt(5 Å)/Co(4 Å)$]_3$/Pt(20 Å) (dotted line), and glass/Pt(100 Å)/$[$Pt(5 Å)/Co(4 Å)$]_3$/Pt(20 Å) (dashed line). Measurements are made using AGFM with the field applied perpendicular to the sample surface.

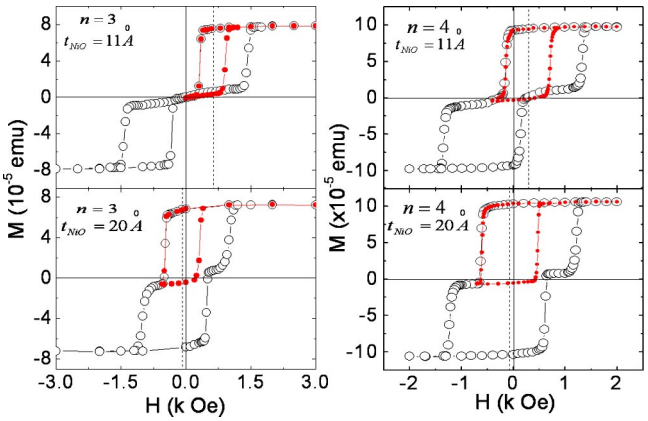

FIG. 3. The major and minor hysteresis loops at room temperature for the samples with NiO thicknesses of 11 and 20 Å in S1 ($n=3$) and S2 ($n=4$), which were measured using SQUID with the applied field along the out-of-plane easy axis. For the measurement of minor loops, a large field was applied first to saturate the whole sample; the field was then decreased until the upper Co/Pt multilayer had reversed direction. Finally, the field was increased again to finish the measurement. During this process, the bottom Co/Pt multilayer remains saturated due to its larger coercivity. The vertical dashed lines in the hysteresis loops give the shifts of the minor loops.

axes, and the absence of a loop shift indicates that there is no exchange bias at room temperature. The Pt/Co multilayer with a NiO overlayer has the highest coercivity (887 Oe) followed by the bare Pt/Co multilayer ($H_c=390$ Oe). The Pt/Co multilayer grown on a NiO layer has the lowest coercivity (80 Oe). The coercivity of magnetic multilayers is known to depend on the deposition parameters of the underlayer, which affects the sample's microstructure leading to differing grain sizes and roughness, which in turn lead to variations in the coercivity. In particular, the effect of interface roughness and coercivity for multilayers with out-of plane anisotropy has been discussed previously.[37–39] In this work, we have not attempted to characterize the degree of roughness, the effect of the microstructure or any other parameters responsible for the differing coercivities. Rather we look upon this as a serendipitous occurrence that enables us to accurately measure the interlayer exchange coupling. If interlayer coupling exists between the two Co/Pt multilayers across the NiO spacer, the coupling can be obtained from a measurement of the minor loop shift of the top multilayer, while the bottom multilayer remains saturated.[19,22]

B. Oscillatory interlayer coupling as a function of NiO thickness

1. Variation of H_{MLS} with NiO thickness

Figure 3 displays the major and minor hysteresis loops at room temperature for samples with NiO thicknesses of $t_{\mathrm{NiO}}=11$ and 20 Å in both S1 and S2. With the exception of a single sample in S2 (at a NiO thickness of 13 Å), all samples in both S1 and S2 display two well separated sharp transitions in the major loop, allowing for easy measurement of

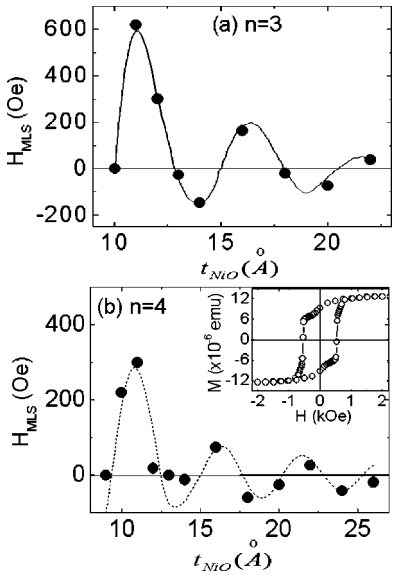

FIG. 4. Variation of the minor loop shift H_{MLS} with the NiO thickness t_{NiO} at room temperature for (a) the samples in S1 with $n=3$ and (b) the samples in S2 with $n=4$. The dotted lines are guides to the eyes. The inset in (b) is the hysteresis loop for a NiO thickness of 13 Å, which displays only one transition. For this sample, a measurement of the minor loop is not possible, and the minor loop shift is simply set to zero, but that does not necessarily indicate that the two Co/Pt multilayers are decoupled.

the minor loop. The coupling strength J_{IEC} can be determined from the minor loop shift H_{MLS} as

$$J_{\mathrm{IEC}} = H_{\mathrm{MLS}} M_S t_{\mathrm{Co}}$$

(see Ref. 22), where M_S and t_{Co} are the saturation magnetization and total thickness of Co layers in the Co/Pt multilayer, respectively.

For the sample in S2 with a NiO thickness of 13 Å, the major loop shown as the inset in Fig. 3(b) displays only one transition, implying that the two Co/Pt multilayers switch together. A possible explanation for this behavior is that the two Co/Pt multilayers are so strongly (ferromagnetically) coupled that they reverse simultaneously. Hence, ferromagnetic coupling may exist between the top and bottom Co/Pt multilayers; however, we set the minor loop shift for this NiO thickness to zero for simplicity in Fig. 4(b). Figures 4(a) and 4(b) show the variations of H_{MLS} with the NiO thickness t_{NiO} for S1 and S2, respectively, at room temperature. Clearly, the IEC at room temperature oscillates between antiferromagnetic and ferromagnetic with a period of ~5 Å for both S1 and S2, but the strength of the coupling is weaker for the S2 sample set. We focus on this difference in Sec. III.

This surprising oscillatory behavior of the interlayer coupling as a function of the NiO thickness is quite different from the nonoscillatory decay of the interlayer coupling strength expected by Bruno's model[27] for nonmagnetic insulating spacers and from experimental observations of coupling across a nonmagnetic insulating MgO spacer in Fe/MgO/Fe systems with in-plane anisotropy.[18] Possible explanations include a modulation of the NiO insulating barrier

by the antiferromagnetic (AFM) ordering[35] and /or exchange coupling at the Co/NiO interfaces.[40] In the quantum interference model by Bruno,[27] the insulating spacer is modeled by a rectangular potential barrier with an height of U_0 higher than the Fermi level E_F of the ferromagnetic layers, and the interlayer coupling is ascribed to the interference of electron waves in the spacer layer due to spin-dependent reflections at the FM/insulator interfaces.[41] Bulk NiO is an insulating antiferromagnet and in our previous work we have argued that the Néel temperature even for such a thin film is at or above room temperature. The period of oscillation corresponds closely to the AF ordering vector, leading to the inescapable conclusion that the oscillatory coupling is closely related to the antiferromagnetic ordering of the NiO samples. Taking the AF ordering of NiO into consideration, a possible explanation for the oscillatory interlayer coupling observed in our system was proposed in a previous paper[35] and is briefly reviewed here.

Assuming that the thin NiO layer in our samples has a spin structure similar to that of the bulk, the (111) texture of the NiO (as revealed by x rays, Fig. 1) implies successive (111) planes of NiO will have net magnetizations pointing in opposite directions, lying parallel to the interfaces. The magnetization of each (111) plane will contribute to the scattering of the spin-polarized electron waves from the FM(111) planes. The presence of domains and different in-plane crystalline orientations in the NiO layer will alter the in-plane direction of the magnetization for differing areas, but the antiferromagnetic ordering of the NiO(111) planes ensures that electron waves traveling through the barrier will experience magnetic fields that are opposite in direction for each successive NiO(111) plane. Rather than a rectangular potential barrier with a width given by the thickness of the spacer (as proposed for nonmagnetic insulating spacers),[27] one may consider a periodic potential $V(z)$ with a period of $2d$ inside the NiO layer (where $d=2.4$ Å is the distance between NiO (111) planes). This periodic potential barrier will cause multiple reflections of electron waves from the FM ordered (111) planes in the NiO layer as well as the Co/NiO interfaces. Their interference may then allow for a modulation of the reflectivity through the NiO by a function which is periodic in the NiO thickness with a period of $2d=4.8$ Å, consistent with the observed oscillatory period of ~ 5 Å.

In the above explanation, the out-of-plane magnetization does not play a significant role, since, according to the model by Slonczewski,[42] it is only the relative orientation of magnetization in the FM layers that is important, which in our case is either parallel or antiparallel to the out-of-plane easy axis. The presence of interfacial roughness will alter the strength of the coupling, since small local regions may display opposite signs for the coupling (for example, some small regions with FM coupling in the AF coupling case). However, so long as a majority of the area of the interface is of the average thickness measured, we still expect to see a net coupling as described above.

An alternative explanation for the coupling has been proposed by Zhuravlev, Tsymbal, and Jaswal.[40] Using a model in which they take into account exchange coupling at the interface and the anisotropy energies of the NiO and Co/Pt multilayers, they are able to reproduce the oscillatory coupling that we have seen.

As described above, the strong (111) texture indicated by the x-ray diffraction implies that the Ni spins are, for the most part, aligned in the plane of the sample, perpendicular to the Co magnetization. In order for exchange coupling to occur at the interface, we expect an out-of-plane canting of the NiO spins. Preliminary evidence of this canting was seen in x-ray magnetic circular dichroism (XMCD) measurements performed at the Advanced Photon Source. XMCD probes the spin-polarized density of states via core-level absorption of circularly polarized x rays, and is sensitive to the projection of the element specific net magnetization along the beam direction. The Ni L3 XMCD data, shown in Figs. 5(a) and 5(b), were taken at remanence after saturation at normal incidence, and thus are sensitive to the out-of-plane component of the Ni magnetization, and not to uncompensated in-plane Ni spins. The data indicate clearly that in the antiferromagnetically coupled sample the net Ni moment is close to zero, whereas in the ferromagnetically coupled sample, a net Ni moment exists. Measurements of the ferromagnetically coupled sample were repeated for saturation in a negative field and showed the opposite sign, as expected. The insets to Fig. 5 indicate a schematic of the possible spin canting in the NiO. Spin canting at one interface is then propagated across the AFM ordered NiO, constraining the direction of canting of the opposite interface. The details of the domain wall in the NiO are not known; the schematic presents only the canting at the interface. In this picture, a FM coupling corresponds to an odd number of NiO layers, whereas AFM coupling occurs with an even number of NiO atomic planes. This is consistent both with our previous data as well as the model of Zhuravlev and co-workers.[40] The canting of the NiO spins seen here does not rule out the earlier explanation; however it does provide strong support for the model of exchange coupling at the interface. The role of the out-of-plane magnetization may be confined to the fact that in-plane magnetization will exchange couple to the in-plane components of the NiO spins which may be randomly arranged, hence leading to a very small or zero net effect. Clearly a detailed study with differing magnetic orientations is necessary.

2. Magnetic force microscopy imaging

The variation of domain formation with NiO thickness provides further insight into the oscillatory IEC. MFM images of as-grown samples show striking differences in the domains of FM and AFM coupled samples. In MFM, the magnetic force gradient from the sample on the tip leads to a phase shift, $\Delta\Phi$, in the oscillatory behavior of the MFM tip. In the point dipole approximation,[43] the phase shift can be expressed simply by $\Delta\Phi=-(Q/k)m_{\mathrm{tip}}\, d^2H_z/dz^2$, where Q and k are the quality factor and the spring constant of the cantilever respectively, m_{tip} is the magnetization of the tip in the dipole approximation, and H_z is the z-component of the stray field above the sample surface. The MFM image is proportional to the intensity plot of $\Delta\Phi$ and in the following we describe and measure this phase shift as an indicator of the presence of domains and domain walls.

Figure 6 shows the MFM images in the as-grown state for four NiO thicknesses in S1. For NiO thicknesses of 11 and

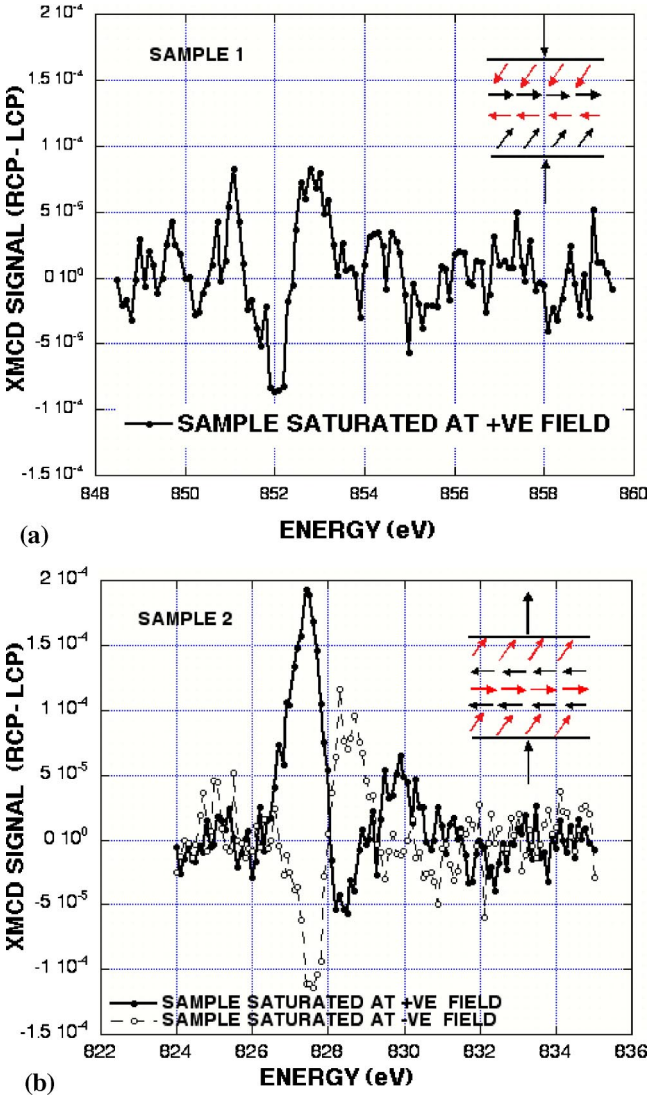

FIG. 5. (Color online) XMCD spectra for (a) an AF coupled sample 1: Si / Pt(100 Å) / [Pt(6 Å) / Co(4 Å)]$_3$ / NiO(11 Å) / [Co(4 Å) / Pt(5 Å)]$_3$ / Pt(24 Å) and (b) ferromagnetically coupled sample 2: Glass/Pt(100 Å) / [Pt(6 Å)/Co(4 Å)]$_3$ / NiO(11 Å) / [Co(4 Å) / Pt(5 Å)]$_3$ / Pt(50 Å). The data shown are the difference between right circularly polarized (RCP) and left circularly polarized (LCP) x rays, a measure of net magnetization. The energy is tuned to the L_3 edge of Ni and the beam is at normal incidence; hence we probe only the out-of-plane component of the Ni magnetization. For sample 2, we show data after both positive and negative saturation; the magnetization clearly displays the opposite sign for positive and negative remanence. The insets are a sketch of the canting of the NiO spins at the interface.

16 Å, (corresponding to AFM coupling), the images in Figs. 6(a) and 6(c) are quite different from the MFM image in Fig. 7(a) for a pure Co/Pt multilayer. In these images, up and down domains disappear, and only closed domain walls are observed. For FM coupled samples with $t_{NiO}=14$ and 18 Å, the domain images shown in Figs. 6(b) and 6(d) are similar to the MFM image in Fig. 7(a) for the pure Co/Pt multilayer. Up and down domains are observed. One other point of observation is that as the NiO thickness grows (and the coupling grows weaker) the *size* of the domains increases. We will attempt to address this phenomenon later in this paper. For now we point out that weaker coupling appears to increase the domain size.

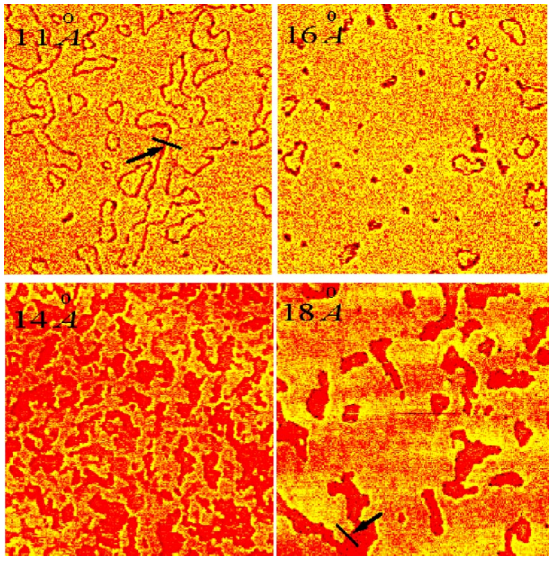

FIG. 6. (Color online) Room temperature MFM images in the as-grown states for samples with NiO thicknesses of 11, 14, 16, and 18 Å in S1. The imaging area is 10 μm$\times$10 μm. For NiO thicknesses of 11 and 16 Å, the interlayer coupling is antiferromagnetic and only closed domain walls are observed, while for the NiO thicknesses of 14 and 18 Å, the interlayer coupling is ferromagnetic and up and down domains are observed, similar to the domain pattern for the pure Co/Pt multilayer shown in Fig. 6.

Figure 7(a) shows an MFM image of a glass/Pt(100 Å)/[Co(4 Å)/Pt(5 Å)]$_3$/Pt(50 Å) multilayer in its as-grown state. The image is composed of areas with light and dark contrasts, corresponding to up and down domains. The schematic diagram above the image in Fig. 7(a) describes $\Delta\Phi$ in the presence of a domain wall when the magnetic moments transition from up to down. On its left is the experimental curve of the phase shift $\Delta\Phi$ across a domain wall from up to down domains. At the bottom of the image in Fig. 7(a), the experimental curve represents the phase shift $\Delta\Phi$ across a domain wall from down to up domains. These two experimental curves of the phase shift $\Delta\Phi$ clearly show opposite signs for up and down domains, as expected.

For two Co/Pt multilayers separated by a thin NiO spacer, both multilayers will generate stray fields above the sample surface. When the magnetic tip scans across the sample surface, the total phase shift, $\Delta\Phi$, is a superposition of two phase shifts

$$\Delta\Phi = \Delta\Phi_{TOP} + \Delta\Phi_{BOTTOM},$$

where $\Delta\Phi_{TOP}$ and $\Delta\Phi_{BOTTOM}$ are the phase shifts caused by the stray fields emanating from the top and bottom Co/Pt multilayers, respectively.

For AFM coupling, the magnetic moments in the two Co/Pt multilayers tend to lie antiparallel. For a down (up) domain in the bottom Co/Pt multilayer, the corresponding coupled domain in the top Co/Pt multilayer must be an up

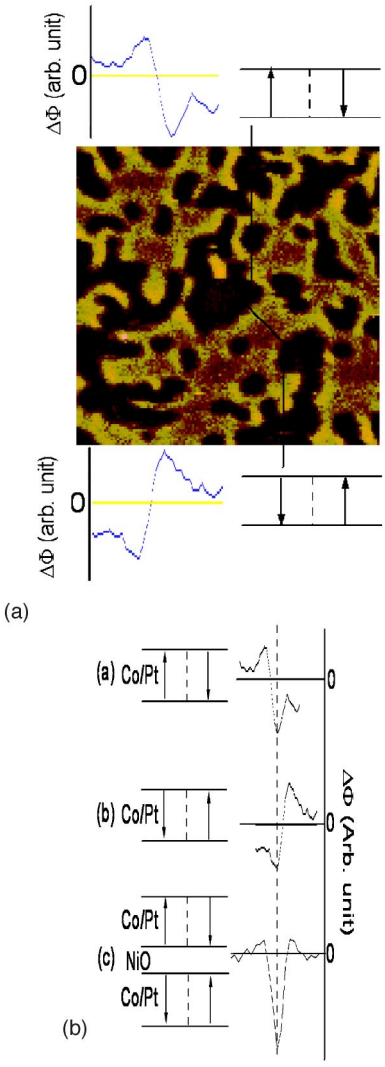

FIG. 7. (Color online) Schematic diagrams to show the formation of closed domain walls in antiferromagnetic coupled Co/Pt multilayers separated by NiO spacers. Figure 7(a) on the left is a MFM image of the domain pattern for glass/Pt(100 Å)/[Pt(5 Å)/Co(4 Å)]$_3$/Pt(20 Å) in the as-grown state. The imaging area is 5 μm$\times$5 μm. The areas with light and dark contrasts correspond to magnetic domains with the moments pointing up and down, respectively. The schematic diagrams on the top and bottom of the image indicate the existence of domain walls between up and down domains, and on their left are the experimental curves of the phase shifts. The experimental curve of the phase shift in (c) is for the domain wall labeled by the solid line in the image with t_{NiO}=11 Å in Fig. 6. The experimental curves in (a) and (b) are from the domain walls labeled by the solid line the Co/Pt layer in the figure on the left.

(down) domain. This guarantees that the magnetic moments in top and bottom Co/Pt multilayers lie antiparallel. The phase shifts caused by the stray fields emanating from the antiferromagnetically coupled up and down domains are opposite in sign and cancel each other to give an average zero phase shift as shown by the experimental curve of the phase shift in Fig. 7(b) and no up and down domains can be observed. However, the phase shifts caused by the domain walls in the top and bottom Co/Pt multilayers do not cancel each other. As shown in Fig. 7(b), their superposition will give a profile of the phase shift similar to that for the domain wall in the antiferromagnetically coupled top and bottom Co/Pt multilayers. Thus, the domain walls observed in the antiferromagnetically coupled Co/Pt multilayers is a superposition of two domain walls from the top and bottom Co/Pt multilayers.

For ferromagnetic interlayer coupling, magnetic moments in the two Co/Pt multilayers lie parallel. For an up (down) domain in the bottom Co/Pt multilayer, the corresponding coupled domain in the top Co/Pt multilayer must be an up (down) domain in order to guarantee parallel alignment of magnetic moments in both coupled Co/Pt multilayers. Thus, in the case of ferromagnetic coupling, up and down domains can be observed. The agreement between the experimental and calculated profiles of $\Delta\Phi$ indicates that the coupling between the top and bottom Co/Pt multilayers occurs domain by domain. Hence only closed domain walls are observed in the antiferromagnetic case, while up and down domains are observed in the ferromagnetic case similar to the pure Co/Pt multilayer.

3. Variation of the antiferromagnetic coupling strength with Pt *thickness*

The strongest antiferromagnetic interlayer exchange coupling occurs for both S1 and S2 when the NiO spacer thickness is 11 Å. Choosing this thickness of 11 Å of NiO, and the number of repeats to be 3, we vary the thickness t_{Pt} of the Pt layers, to make a series of samples, S3, to check the variation of the antiferromagnetic coupling strength with Pt thickness t_{Pt}.

Figure 8 displays the major and minor loops for samples in S3. All minor loops demonstrate a net positive shift, implying that the coupling remains antiferromagnetic at all Pt thicknesses. The MFM images in Fig. 9 show the closed domain walls expected for antiferromagnetic interlayer coupling between the top and bottom Co/Pt multilayers, further confirming the antiferromagnetic coupling feature. Once again, increasing the Pt thickness (and hence decreasing the coupling strength) leads to the formation of larger domains. In general, domain formation is a balance between anisotropy energies and magnetostatic energy, where the domain wall energies depend on the anisotropy. If the exchange coupling can be thought of as an effective anisotropy [see Eq. (5) below], as the exchange coupling decreases, it should be *easier* to form domains, leading to smaller domain sizes to minimize the magnetostatic energy. Alternatively, we can consider the coupling between layers to provide an effective field; the stronger the coupling, the larger the field and hence the larger the domain size. Our observation of increased domain size as a function of decreased coupling strength runs counter to the arguments given above. A similar effect has been seen in Co/Pt multilayers, albeit with larger Co thickness by Stamps *et al.*[44] Calculations of domain size in multilayers with out-of-plane anisotropy have been performed;[45] these calculations consider only magnetostatic interactions between the magnetic layers and do not consider the dependence of domain size on spacer layer thickness or coupling

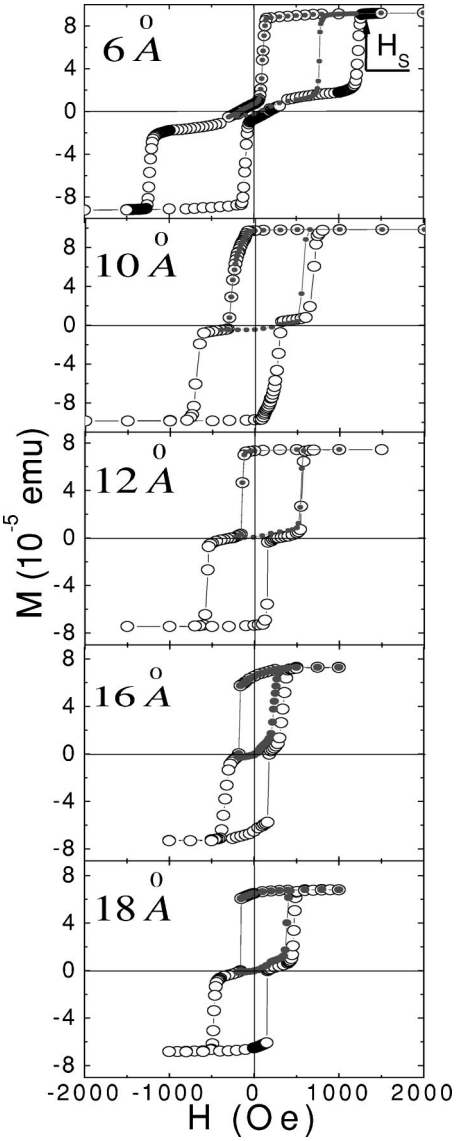

FIG. 8. The major and minor hysteresis loops for samples with differing Pt thicknesses in S3. The numbers represent the Pt thickness. A switching field H_{SW} is defined as shown in the hysteresis loop with Pt thickness of 6 Å, being the field at which the lower Co/Pt multilayer reverses completely.

strength. For Fe/Cr/Fe sandwiches with in-plane magnetization, both calculations (assuming only Néel walls are present) and experiment[46] show that the domain wall widths *increase* with decreasing coupling strength. However, in our films with out-of-plane anisotropy, Bloch-type domain walls are probable. Calculations of domain effects for out-of-plane thin films with IEC have not been performed.

In the major loop, a switching field H_{SW} is defined as shown in Fig. 8(a), corresponding to the field at which the entire lower Co/Pt multilayer switches magnetization. The variation of the switching field, H_{SW} and the minor loop shift, H_{MLS} as a function of Pt thickness are shown in Figs. 10(a) and 10(b), respectively. H_{SW} decays exponentially with Pt thickness and the best fit shown as a solid line in the figure is given by

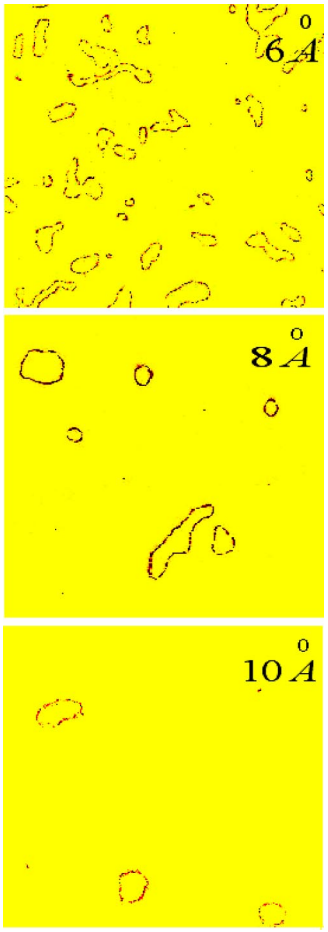

FIG. 9. (Color online) Room temperature MFM images at the as-grown state for the samples with the thicknesses of t_{Pt}=6, 8, and 10 Å in S3. The imaging area is 20 μm$\times$20 μm. Only closed domain walls are observed in these samples, suggestive of antiferromagnetic interlayer coupling between the top and bottom Co/Pt multilayers. The domain size increases with increasing Pt thickness.

$$H_{SW} = 198.3 + 2665.8e^{-0.15t_{Pt}}.$$

H_{MLS} shows a decaying oscillatory dependence on Pt thickness, that on fitting can be best described by

$$H_{MLS} = 8.31 + 336.92e^{-0.15\ t_{Pt}} - 80.12\ \sin(1.12(-t_{Pt}2.88)).$$

In order to understand the striking similarity of the exponential factors of H_{SW} and H_{MLS}, with increasing Pt thickness, we need to consider the effects of decreased coupling strength across the Co layers. Let us consider a single Co/Pt multilayer with perpendicular anisotropy. The perpendicular anisotropy arises from an interface anisotropy, and the anisotropy energy can be expressed as $K_S \cos^2 \vartheta$, where $K_S > 0$ is the interface anisotropy constant, and ϑ is the angle between the magnetization and the interface normal. A variety of experimental studies[47–49] have shown the existence of ferromagnetic coupling in Co/Pt multilayers. If a magnetic field H is applied perpendicular to the interface, the total energy per unit area can be written as[50]

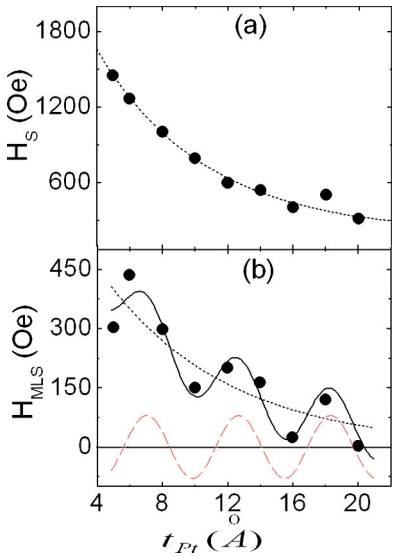

FIG. 10. (Color online) Variations of the (a) switching field H_{SW}. The dotted line is the fit to the data showing the exponential decay of H_{SW} with t_{Pt} and (b) the minor loop shift H_{MLS} as a function of the Pt thickness t_{Pt}. The solid line is a fit to the data, showing that the variation of H_{MLS} with t_{Pt} is a superimposition of an oscillation with period of ~6 Å (dashed line) onto an exponential decay (dotted line).

$$E = -(K_S - 2\pi M_S^2)\cos^2\vartheta - M_S H\cos\vartheta + E_{ex}, \qquad (1)$$

where M_S is the saturation magnetization of the Co layer, $2\pi M_S^2$ is the magnetostatic energy. E_{ex} is the exchange coupling energy between Co layers and ϑ is the angle of the magnetization with respect to the applied field. This definition of ϑ is based on the assumption that all magnetic moments are parallel. If we consider only two Co layers separated by a Pt layer, E_{ex} can be expressed as[43]

$$E_{ex} = -J_{ex}\mathbf{m}_1 \cdot \mathbf{m}_2 \qquad (2)$$

where J_{ex} is the exchange coupling constant and $\mathbf{m}_1$ and $\mathbf{m}_2$ are the unit vectors of the magnetizations in the two Co layers. Equation (2) is the generalization of the Heisenberg-type isotopic exchange to the interlayer problem, and the generalization is based on the assumption that the ferromagnetic layer is in a single domain. Equation (3) can be further expanded as

$$E_{ex} = -J_{ex}\{\cos\vartheta_1\cos\vartheta_2 + \sin\vartheta_1\sin\vartheta_2\cos(\phi_1 - \varphi_2)\}, \qquad (3)$$

where $\vartheta_{1,2}$ is the angle between $\mathbf{m}_{1,2}$ and $\mathbf{H}$, and $\varphi_{1,2}$ is the azimuthal angle of $\mathbf{m}_{1,2}$. The magnetic field $\mathbf{H}$ limits the value of $\vartheta_{1,2}$ and the sharp transition in the hysteresis loop (see Fig. 2) implies that the Co layers reverse simultaneously; hence the assumption that $\vartheta_1 = \vartheta_2$ is valid. The azimuthal angles, φ_1 and φ_2, are not confined by the field, may vary from grain to grain and are susceptible to extrinsic effects. Averaging over the area of the surface $\langle\cos(\varphi_1 - \varphi_2)\rangle$ will tend to zero since there is no preferred orientation in plane. We can then rewrite Eq. (3) as

$$E_{ex} = -J_{ex}\cos^2\vartheta \qquad (4)$$

and substitute this into the free energy equation

$$E = -(K_S + J_{ex} - 2\pi M_S^2)\cos^2\vartheta - M_S H\cos\vartheta. \qquad (5)$$

On the assumption that the domain size of the Co/Pt multilayer is large [the condition which our samples satisfy (see Fig. 9)], the switching field H_{SW} can be determined by[50]

$$H_{SW} = 2\frac{K_{eff}}{M_S}, \qquad (6)$$

where $K_{eff} = K_S + J_{ex} - 2\pi M_S^2$. H_{SW} is controlled by three parameters: the interface anisotropy constant K_S, the saturation magnetization, and the interlayer coupling constant J_{ex}. Neither K_S nor M_S are influenced by a change in the Pt thickness. Hence, the exponential decay of H_{SW} with increasing Pt thickness must be ascribed to the exchange coupling constant. Experimental studies[49] have demonstrated that in Co/Pt multilayers, J_{ex} decays exponentially with increasing Pt thickness, consistent with our observed exponential decay of H_{SW}.

The connection between the IEC and the switching field is more subtle. A measurement of the minor loop is only possible when one Co/Pt multilayer (in this case the lower one) remains saturated. With increasing Pt thickness, the exponential decay of H_{SW} for the lower Co/Pt multilayer implies that the field range over which the lower multilayer can remain saturated will become increasingly narrow. The upper limit for the minor loop shift of the top Co/Pt multilayer is H_{SW}. Hence, the exponential-decay contribution to the interlayer exchange coupling may be ascribed to the exponential decay of the exchange coupling constant J_{ex}.

The oscillatory component is periodic with a period of ~6 Å. This oscillatory behavior as a function of t_{Pt} is similar to that observed in FM/metallic spacer/FM systems[28,29] as a function of the FM layer thickness. According to the quantum interference model by Bruno,[27] the entire multilayer may be represented by a series of potential barriers. Due to multiple reflections from the two interfaces of the FM layer and their interference, oscillation of the coupling strength as a function of the FM layer thickness is expected. In our case, the FM layer is composed of the Co/Pt multilayers. Thus, following Bruno[25,27] and Stiles,[26] the Co/Pt multilayers can be represented by a sequence of potential barriers or quantum wells. The coupling strength is determined by the spin dependent reflectivity of electron waves at the Co/Pt interfaces, which, in turn, is determined by the interference effects due to the partial reflection and transmission of electron waves at the Co/Pt interfaces. Increasing t_{Pt} leads to the increase of the well width between the potential barriers. As a result, an oscillation of the coupling strength with t_{Pt} is expected. This oscillation is superimposed onto the exponential decay of the AF coupling strength as a function of t_{Pt} caused by the exponential decay of the coupling strength between Co layers across the Pt layers.

4. Variation of the antiferromagnetic coupling strength with n

For the strongest antiferromagnetic interlayer coupling at the NiO thickness of 11 Å in S1, the variation of the cou-

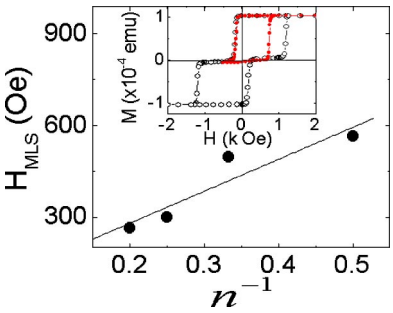

FIG. 11. (Color online) Linear dependence of the minor loop shift H_{MLS} on $1/n$ in S4 where n is the number of repetitions of the Co/Pt multilayer. The solid line is the linear fit to the experimental data (solid dots). The inset shows the major and minor hysteresis loops for the sample with $n=5$ in S4.

pling strength as a function of n (the number of repetitions of the Co/Pt multilayer) has been investigated. The inset in Fig. 11 gives the major and minor loops for $n=5$. The net positive minor loop shift indicates antiferromagnetic interlayer coupling. Figure 11 shows a linear increase of the antiferromagnetic coupling strength with $1/n$. This linear dependence on $1/n$ (or $1/d$ where d is the total thickness of the magnetic Co/Pt layer) is suggestive of the nature of a surface or interface interaction for the interlayer exchange coupling between Co/Pt multilayers separated by a NiO layer, an observation that is consistent with the XMCD data suggesting the presence of exchange coupling at the interface.

IV. SUMMARY

In summary, the interlayer exchange coupling between two Co/Pt multilayers with perpendicular anisotropy separated by NiO layers has been investigated. The interlayer coupling oscillates between antiferromagnetic and ferromagnetic as a function of the NiO spacer thickness with a period of ~5 Å or 2 ML of the NiO(111) planes. XMCD data indicate a canting of the NiO spins into the out-of-plane direction, suggesting that exchange coupling at the Co/NiO interface plays a role in this oscillatory coupling. The MFM images at different NiO thicknesses have shown that the coupling between the two Co/Pt multilayers occurs domain by domain. For antiferromagnetic coupling, only closed domain walls are observed, which arise from the superposition of domain walls from the top and bottom Co/Pt multilayers. For ferromagnetic coupling, up and down domains are observed, similar to the domain patterns for a bare Co/Pt multilayer. For the strongest antiferromagnetic coupling at a NiO thickness of 11 Å, the variation of the coupling strength with the thickness of the Pt layer is a superposition of an oscillation with a period of 6 Å onto an exponential decay. The exponential decay of the antiferromagnetic coupling strength with the Pt thickness is attributed to the exponential decay of the ferromagnetic coupling constant between the Co layers across the Pt layer in a Co/Pt multilayer, while the oscillatory behavior is ascribed to multiple reflections of electron waves from the Co/Pt interfaces and their interference. Finally, a linear dependence of the antiferromagnetic coupling strength on $1/n$ has been observed, which is suggestive of a surface or interface interaction for the interlayer exchange coupling between two Co/Pt multilayers separated by NiO layers.

ACKNOWLEDGMENTS

We would like to thank Professor Minglang Yan, Professor S. Jaswal, and Professor E. Tsymbal for stimulating discussions regarding the data. This work was supported by NSF9806308 and MRSEC2505210081009. Use of the Advanced Photon Source was supported by the U.S. Department of Energy, Office of Science, Office of Basic Energy Sciences, under Contract No. W-31-109-ENG-38.

*Electronic address: sadenwal@unlserve.unl.edu

[1] P. Grunberg, R. Schreiber, Y. Pang, M. B. Brodsky, and H. Sowers, Phys. Rev. Lett. **57**, 2442 (1986).
[2] S. S. P. Parkin, N. More, and K. P. Roche, Phys. Rev. Lett. **64**, 2304 (1990).
[3] M. E. Brubaker, J. E. Mattson, C. H. Sowers, and S. D. Bader, Appl. Phys. Lett. **58**, 2306 (1991).
[4] Z. Celinski and B. Heinrich, J. Magn. Magn. Mater. **99**, L25 (1991).
[5] S. S. P. Parkin, Phys. Rev. Lett. **67**, 3598 (1991).
[6] A. Cebollada, J. L. Martinez, J. M. Gallego, J. J. de Miguel, R. Miranda, S. Ferrer, F. Batallan, G. Fillion, and J. P. Rebouillat, Phys. Rev. B **39**, 9726 (1989).
[7] W. R. Bennett, W. Schwarzacher, and W. F. Egelhoff, Jr., Phys. Rev. Lett. **65**, 3169 (1990).
[8] J. J. de Miguel, A. Cebollada, J. M. Gallego, R. Miranda, C. M. Schneider, P. Schuster, and J. Kirschner, J. Magn. Magn. Mater. **93**, 1 (1991).
[9] M. T. Johnson, S. T. Purcell, N. W. E. McGee, R. Coehoorn, J. aan de Stegge, and W. Hoving, Phys. Rev. Lett. **68**, 2688 (1992).
[10] A. Fuss, S. Demokritov, P. Grunberg, and W. Zinn, J. Magn. Magn. Mater. **103**, L221 (1992).
[11] S. S. P. Parkin, A. Mansour, and G. P. Felcher, Appl. Phys. Lett. **58**, 1473 (1991).
[12] S. Demokritov, J. A. Wolf, P. Grunberg, and W. Zinn, MRS Symposia Proceedings (Materials Research Society, Pittsburgh, 1992), Vol. 231, p. 133.
[13] J. Unguris, R. J. Celotta, and D. T. Pierce, Phys. Rev. Lett. **67**, 140 (1991).
[14] S. T. Purcell, W. Folkerts, M. T. Johnson, N. W. E. McGee, K. Jager, J. Aan de Stegge, W. P. Zeper, and P. Grunberg, Phys. Rev. Lett. **67**, 903 (1991).
[15] M. Ruhrig, R. Schafer, A. Hubert, R. Mosler, J. A. Wolf, S. Demokritov, and P. Grunberg, Phys. Status Solidi A **125**, 635 (1991).

[16] S. T. Purcell, M. T. Johnson, N. W. E. McGee, R. Coehoorn, and W. Hoving, Phys. Rev. B **45**, 13 064 (1992).
[17] S. S. Yan, R. Schreiber, F. Voges, C. Osthover, and P. Grunberg, Phys. Rev. B **59**, R11 641 (1999).
[18] E. Popova, J. Faure-Vincent, C. Tiusan, C. Bellouard, H. Fischer, E. Snoeck, M. Hehn, F. Montaigne, V. da Costa, M. Alnot, S. Andrieu, and A. Schuhl, Appl. Phys. Lett. **81**, 509 (2002).
[19] J. Faure-Vincent, C. Tiusan, C. Bellouard, E. Popova, M. Hehn, F. Montaigne, and A. Schuhl, Phys. Rev. Lett. **89**, 107206 (2002).
[20] S. Toscano, B. Briner, H. Hopster, and M. Landolt, J. Magn. Magn. Mater. **114**, L6 (1992).
[21] B. Briner and M. Landolt, Europhys. Lett. **28**, 65 (1994).
[22] P. Walser, M. Hunziker, T. Speck, and M. Landolt, Phys. Rev. B **60**, 4082 (1999).
[23] A. Fert and P. Bruno, in *Ultrathin Magnetic Structures*, edited by B. Heinrich and J. A. C. Bland (Springer, Berlin, 1994), Vol. 2, Chap. 2.2, p. 82.
[24] J. C. Slonczewski, J. Magn. Magn. Mater. **150**, 13 (1995).
[25] P. Bruno and C. Chappert, Phys. Rev. Lett. **67**, 1602 (1991); **67**, 2592(E) (1991); **46**, 261 (1992).
[26] M. D. Stiles, Phys. Rev. B **48**, 7238 (1993).
[27] P. Bruno, Phys. Rev. B **52**, 411 (1995).
[28] P. J. H. Bloemen, M. T. Johnson, M. T. H. van de Vorst, R. Coehoorn, J. J. de Vries, R. Jungblut, J. aan de Stegge, A. Reinders, and W. J. M. de Jonge, Phys. Rev. Lett. **72**, 764 (1994).
[29] S. N. Okuno and K. Inomata, Phys. Rev. Lett. **72**, 1553 (1994).
[30] F. Ernult, B. Dieny, and J. R. Regnard, J. Magn. Magn. Mater. **242-245**, 515 (2002).
[31] J. Camarero, Y. Pennec, J. Vogel, M. Bonfim, S. Pizzini, F. Ernult, F. Fettar, F. Garcia, F. Lancon, L. Billard, B. Diney, A. Tagliaferri, and N. B. Brooks, Phys. Rev. Lett. **91**, 027201 (2003).
[32] K. Ounadjela, D. Muller, A. Dinia, A. Arbaoui, P. Panissod, and G. Suran, Phys. Rev. B **45**, 7768 (1992).
[33] S. Hamada *et al.*, J. Magn. Magn. Mater. **240**, 539 (2002).
[34] G. Gubbiotti *et al.*, J. Magn. Magn. Mater. **240**, 461 (2002).
[35] Z. Y. Liu and S. Adenwalla, Phys. Rev. Lett. **91**, 037207 (2003).
[36] D. Alders, L. H. Tjeng, F. C. Voogt, T. Hibma, G. A. Sawatzky, C. T. Chen, J. Vogel, M. Sacchi, and S. Iacobucci, Phys. Rev. B **57**, 18 (1998).
[37] H. S. Oh and S. K. Joo, IEEE Trans. Magn. **32**, 4061 (1996).
[38] Q. Meng, P. de Haan, W. P. van Drent, J. C. Lodder, and Th. J. A. Popma, IEEE Trans. Magn. **32**, 4064 (1996).
[39] T. K. Hatwar and C. F. Brucker, IEEE Trans. Magn. **31**, 3256 (1995).
[40] M. Ye. Zhuravlev, E. Y. Tsymbal, and S. S. Jaswal, Phys. Rev. Lett. **92**, 219703 (2004).
[41] E. Bruno and B. L. Gyorffy, J. Magn. Magn. Mater. **121**, 322 (1993).
[42] J. C. Slonczewski, Phys. Rev. B **39**, 6995 (1989).
[43] D. Rugar, H. J. Mamin, P. Guethner, S. E. Lambert, J. E. Stern, I. McFadyen, and T. Yogi, J. Appl. Phys. **68**, 1169 (1990).
[44] R. L. Stamps, L. Louail, M. Hehn, M. Gester, and K. Ounadjela, J. Appl. Phys. **81**, 4751 (1997).
[45] H. J. G. Draaisma and W. J. M. de Jonge, J. Magn. Magn. Mater. **62**, 3318 (1987).
[46] M. Ruhrig and A. Hubert, J. Magn. Magn. Mater. **121**, 330 (1993).
[47] A. Murayama, M. Miyamura, K. Nishiyama, K. Miyata, and Y. Oka, J. Appl. Phys. **69**, 5661 (1991).
[48] Z. Zhang, P. E. Wigen, and S. S. P. Parkin, J. Appl. Phys. **69**, 5649 (1991).
[49] M. Vohl *et al.*, J. Magn. Magn. Mater. **93**, 403 (1991).
[50] W. J. M. de Jonge, P. J. H. Bloemen, and F. J. A. den Broeder, in Ref. 23, Vol. 1, Chap. 2.2, p. 65.